

Supporting Information

Acid-Base Chemistry at the Single Ion Limit

Vignesh Sundaresan¹ and Paul W. Bohn^{1,2*}

¹Department of Chemical and Biomolecular Engineering, University of Notre Dame, Notre Dame, IN 46556 USA

²Department of Chemistry and Biochemistry, University of Notre Dame, Notre Dame, IN 46556 USA

*Author to whom correspondence should be addressed, pbohn@nd.edu

1. Experimental section

Chemicals and Materials

Fluorescein sodium salt (BioReagent), potassium nitrate ($\geq 99.0\%$), sodium phosphate dibasic heptahydrate (ACS Reagent, 98.0%), sodium phosphate monobasic monohydrate (ACS Reagent, $\geq 98.0\%$), nitric acid (ACS Reagent, $\geq 90.0\%$), and sodium hydroxide (BioXtra, $\geq 98.0\%$) were purchased from Sigma-Aldrich. Alexa Fluor 488 Carboxylic Acid, tris(triethylammonium) salt was purchased from ThermoFisher Scientific. A two-part silicone elastomer (SYLGARD 184) for making polydimethylsiloxane (PDMS) wells was purchased from Fisher Scientific. Glass coverslips (Nexterion Uncoated High-Performance 1.5H Coverslips, Glass D263) were purchased from Applied Microarrays. Conductive silver epoxy (Electrically/Thermally Conductive Bond 556) was purchased from Electron Microscopy Sciences. Ag and Pt wires were purchased from Sigma-Aldrich to make quasi-reference and counter electrodes respectively. All reagents were used without further purification.

Fabrication of E-ZMW devices

The process-flow for fabrication of E-ZMW devices is shown schematically in **Figure S1**. First, a 10 nm thick titanium adhesion layer followed by a 200 nm thick gold film were deposited by electron-beam evaporation on a clean glass coverslip through a custom-made shadow mask. Next, a 100 nm thick SiO₂ layer was deposited on top of the gold film using plasma-enhanced chemical vapor deposition (PECVD). Finally, a dual-source scanning electron microscopy-focused ion beam (SEM-FIB) instrument was used to mill and characterize the E-ZMW devices. FIB parameters were 30 kV acceleration, 0.26 nA ion current, 100 μ s dwell time, and 2 nm Z-depth

to fabricate E-ZMW arrays with the interpore distance of 2 μm . The fabricated devices were rinsed with a copious amount of DI water, then used for the correlated optical and electrochemical experiments.

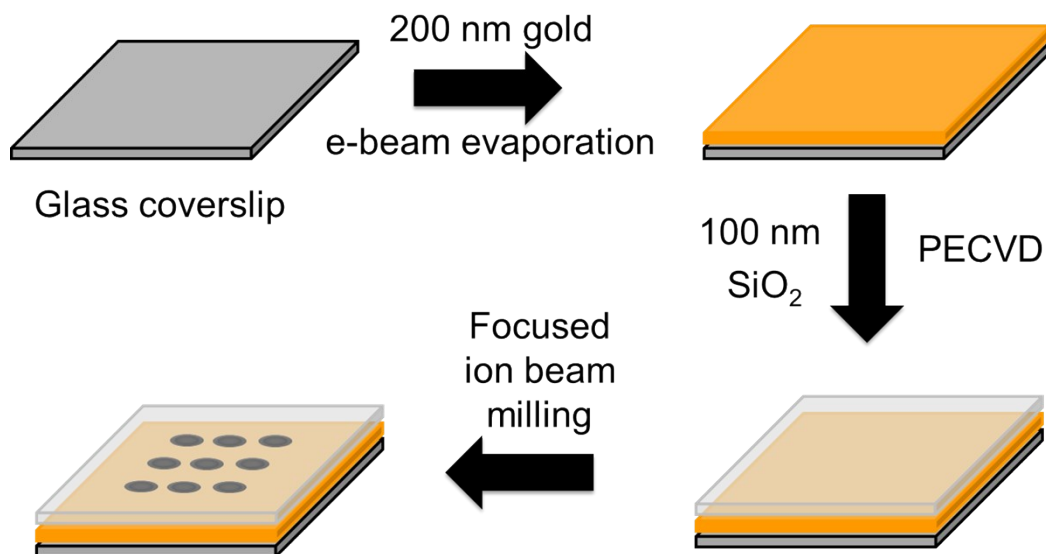


Figure S1. Schematic illustration showing fabrication of electrochemical zero-mode waveguides (E-ZMWs).

Apparatus

The spectroelectrochemical cell was prepared by attaching a copper wire to the E-ZMW device using electrically conductive silver epoxy. Then a 6 mm diam. PDMS well was attached on top to act as an electrolyte reservoir. Pt and Ag/AgCl wires were inserted into the PDMS well to serve as the counter and quasi-reference electrodes, respectively. All electrodes were connected to a potentiostat (CH750E, CH Instruments). The spectroelectrochemical cell was mounted on top of an inverted optical microscope (Olympus IX-71) equipped with a 100 \times objective (Olympus oil immersion, NA 1.45). A 458 nm laser (OBIS, Coherent) was used to excite fluorescence in the solution, and the emission was collected through the objective and imaged onto an EM-CCD

camera (Andor iXon EMCCD camera) after passing through a dichroic cutoff filter. A schematic diagram of the experimental apparatus is shown in **Figure 1** of the main text. CCD camera images were acquired with an acquisition time of 0.1 s per frame.

Image processing

The collected EM-CCD images were analyzed using ImageJ software. The intensity-time traces of individual E-ZMWs were obtained by taking the average intensity of 10 x 10 image pixel areas using the ROI Manager option in ImageJ.

2. Supporting Figures

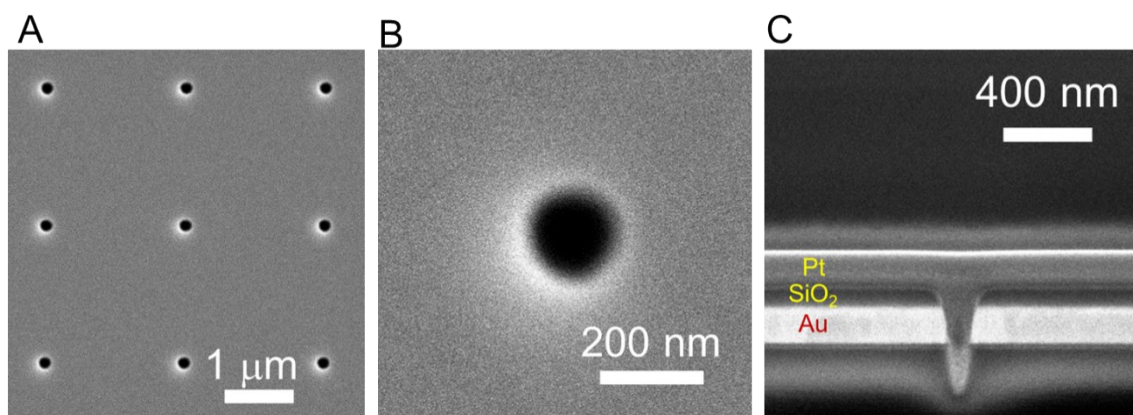


Figure S2. (A) Scanning electron microscopy (SEM) image of 3 X 3 E-ZMWs. (B) Magnified view of one of the pores from panel (A). (C) Cross-sectional SEM view of single pore showing stacked 200 nm thick Au and 100 nm thick SiO₂ layers. Pt was added to enable cross-sectional imaging.

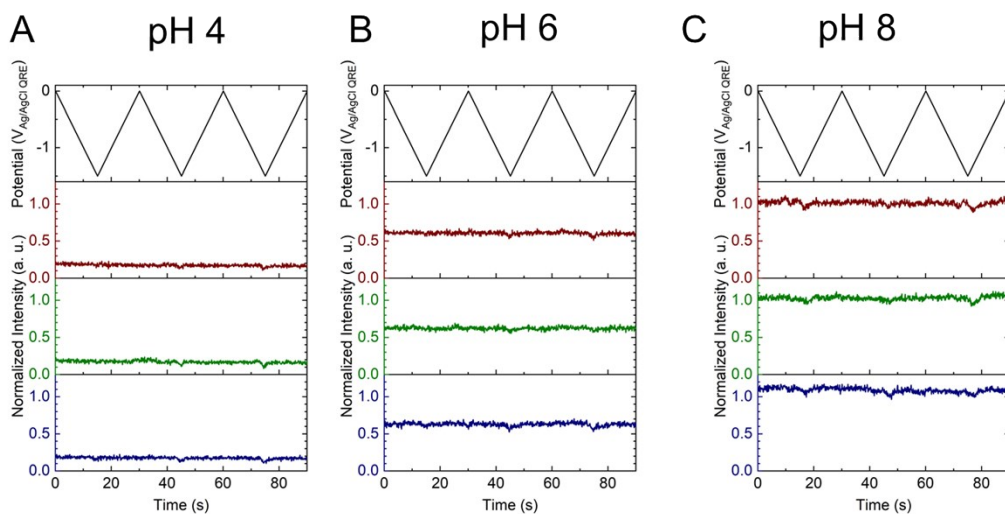


Figure S3. Applied potential waveform as a function of time (top panels) and corresponding individual fluorescence normalized intensity – time traces (bottom panels) for 3 different E-ZMWs with the starting buffer solution of (A) pH 4, (B) pH 6, and (C) pH 8 with 3 μ M fluorescein.

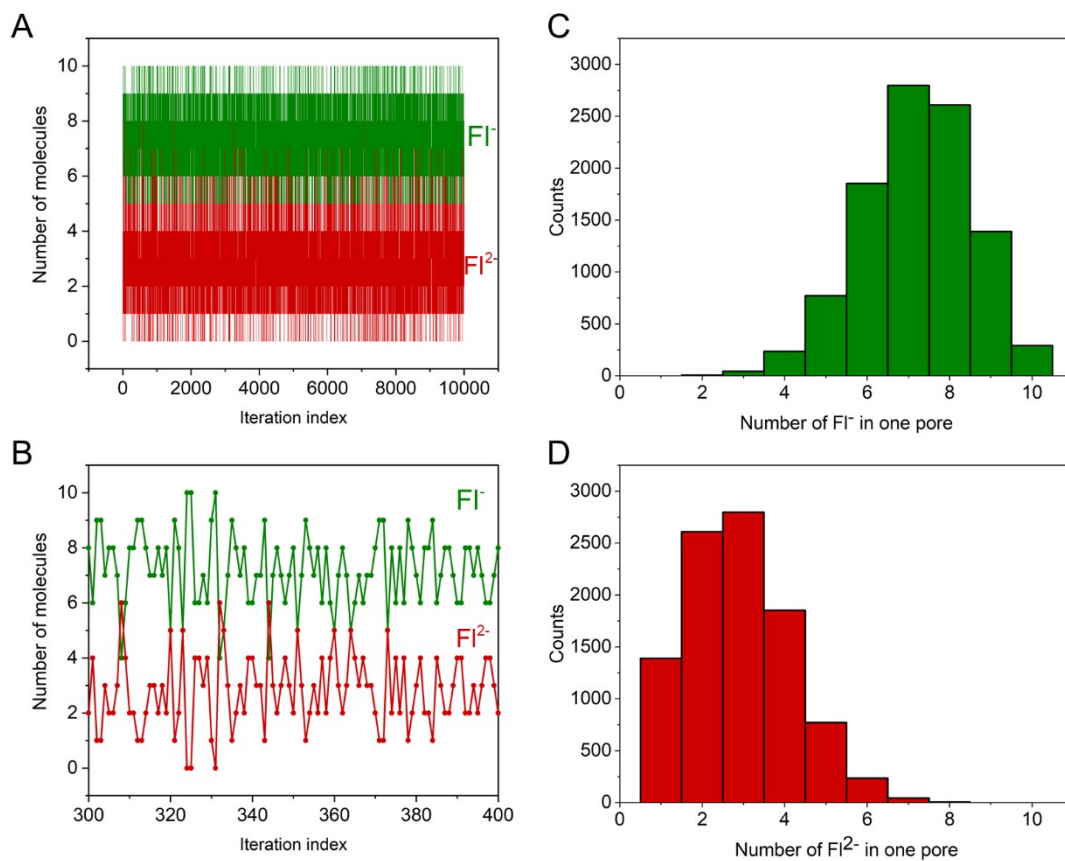


Figure S4. Results of a Monte Carlo simulation with 10000 iterations at pH 6. (A) Number of FI⁻ and FI²⁻ molecules present in single E-ZMW nanopore as a function of iteration index. (B) Magnified view of iteration index 300 to 400 from panel (A). Histogram of number of FI⁻ (C) and FI²⁻ (D) molecules in a single E-ZMW nanopore obtained from Monte Carlo simulation.

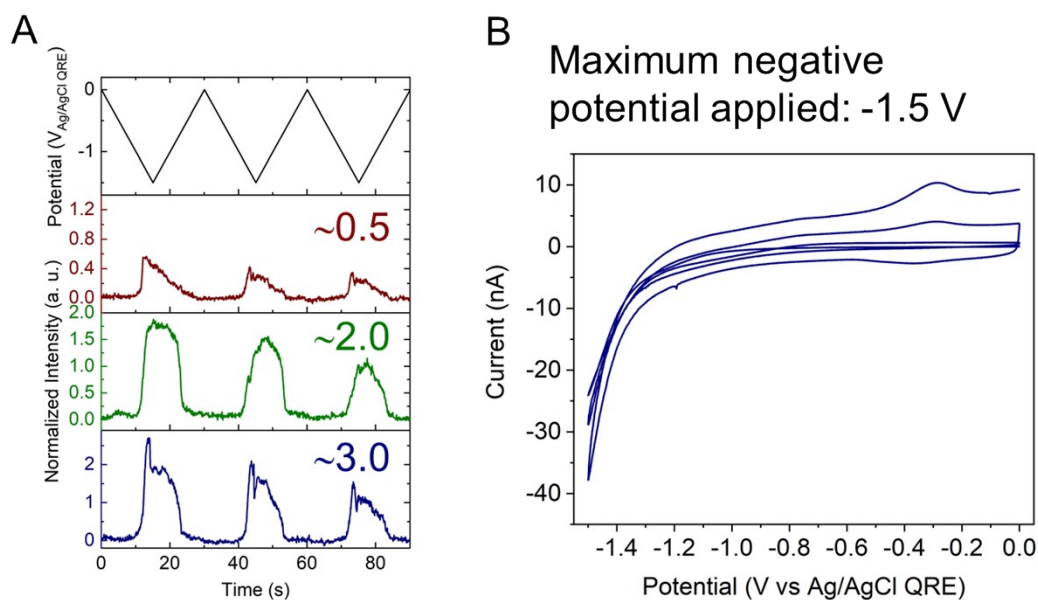


Figure S5. (A) Applied potential waveform as a function of time (*top*) and corresponding fluorescence normalized intensity – time plots (*bottom*) for 3 different E-ZMW nanopores. Each intensity-time plot is labeled with the maximum I_{norm} value observed. Initial conditions were pH 3 with 3 μ M fluorescein and 0.2 M KNO₃. (B) Corresponding cyclic voltammetry current response in the range $0.0 > E_{appl} > -1.5$ V vs. Ag/AgCl acquired at 0.1 V s^{-1} .

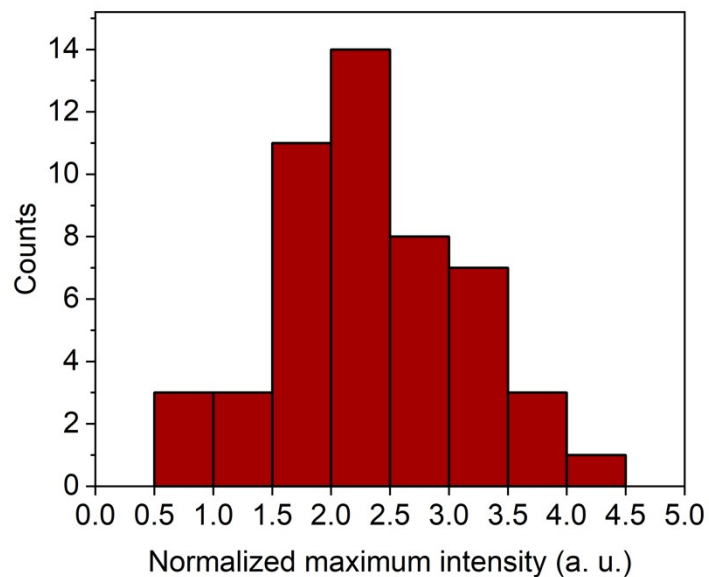


Figure S6. Histogram of maximum I_{norm} values obtained from 50 different E-ZMWs during potential scans in the range $0.0 \text{ V} > E_{appl} > -1.5 \text{ V}$. The intensity scale is matched to that of **Figure 2** of the main text.

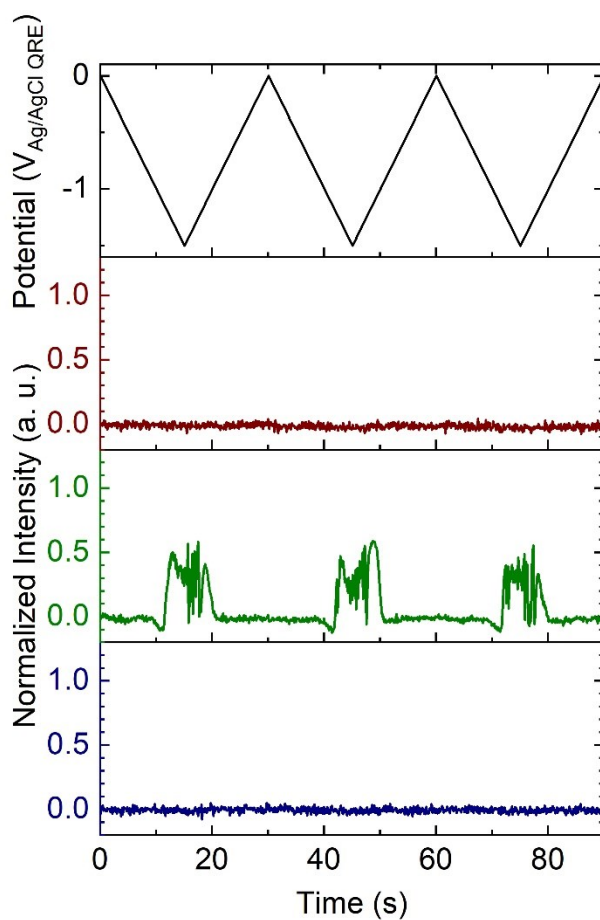


Figure S7. Applied potential waveform as a function of time (*top*) and corresponding individual fluorescence normalized intensity – time traces (*bottom*) for 3 different E-ZMW nanopores.

Experiments are carried out in 0.1 M phosphate buffer solution at pH 3 with 3 μM fluorescein.

Model for anomalous fluorescence emission

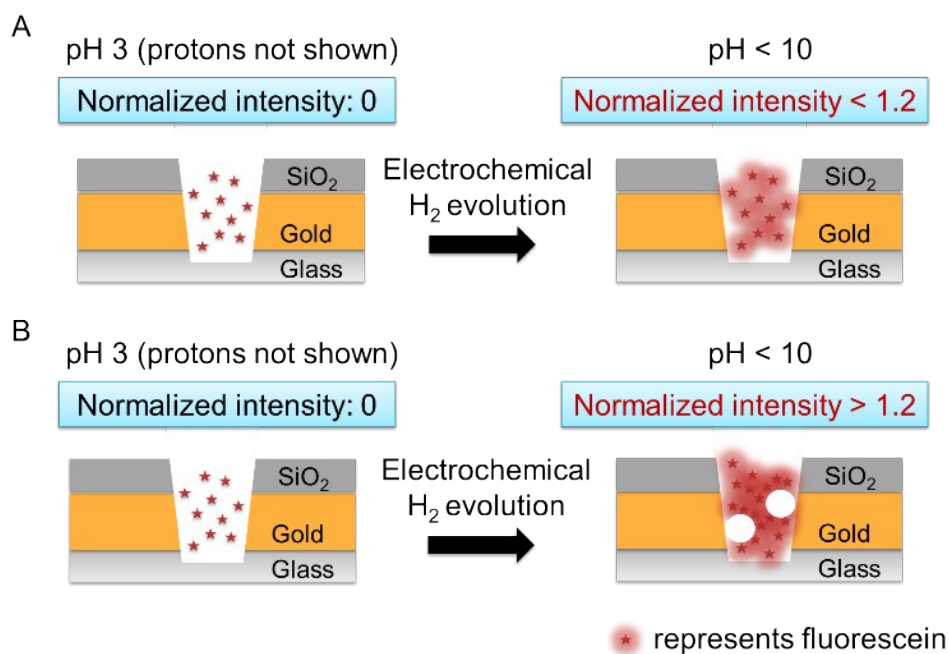


Figure S8. Schematic diagram illustrating the H₂ nanobubble formation hypothesis. In cases where nanobubbles do not form (A), I_{norm} is determined by the acid-base chemistry inside the nanopore and the $F1/F1^{2-}$ ratio. In cases where nanobubbles form (B), I_{norm} is enhanced by a combination of adsorption at the H₂/solution interface and enhanced outcoupling effects.

Fluorescein intensity – pH calibration curve using Pt-based E-ZMWs

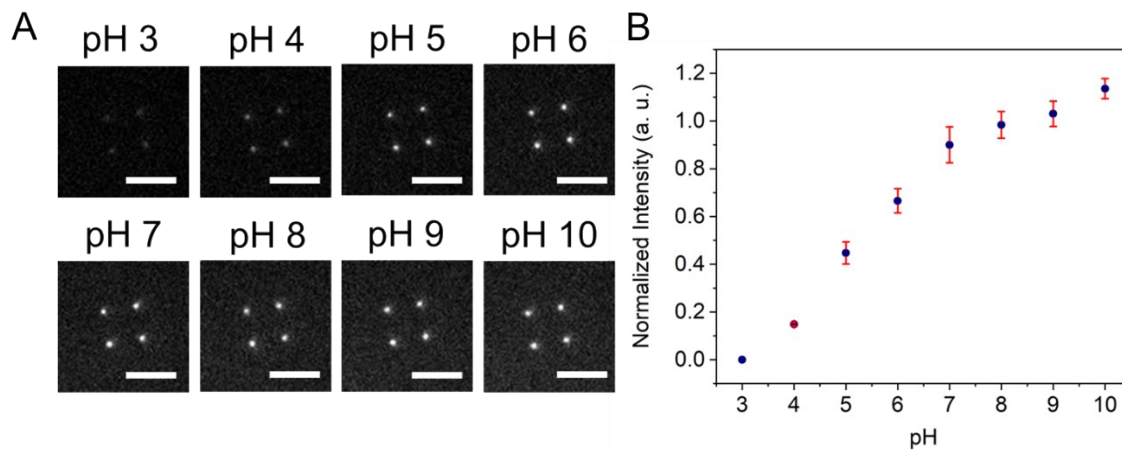


Figure S9. (A) Wide-field fluorescence images of 3 μM fluorescein as a function of pH in 2 X 2 Pt-based E-ZMW arrays. Scale bars are 4 μm . (B) Calibration curve showing normalized fluorescence intensity as a function of solution pH. Laser intensity: 176 W/cm^2 .

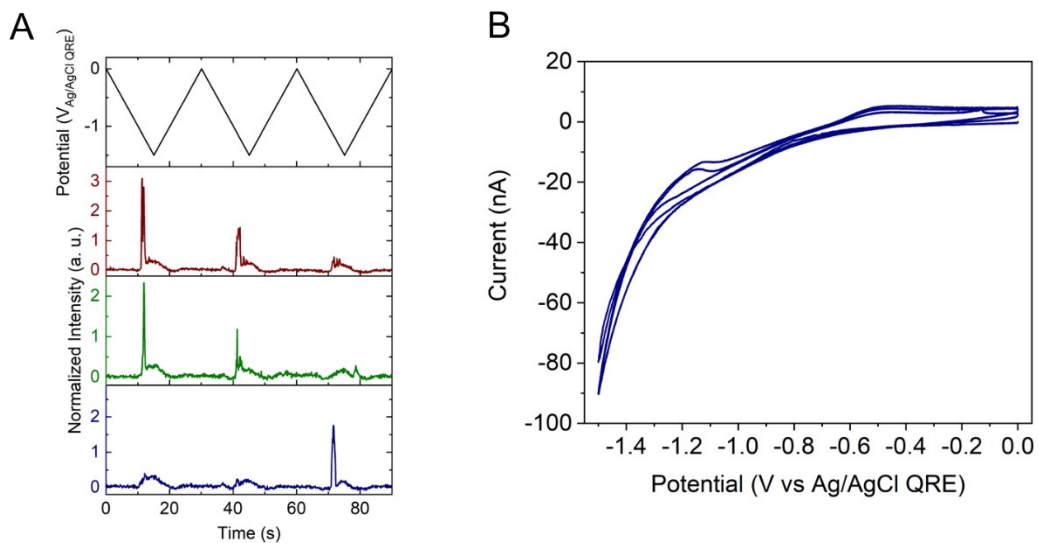


Figure S10. (A) Applied potential waveform as a function of time (*top*) and corresponding individual fluorescence normalized intensity – time traces (*bottom*) for 3 different Pt-based E-ZMW nanopores. The initial pH of the solution is pH 3 with 3 μ M fluorescein and 0.2 M KNO_3 . (B) Corresponding cyclic voltammetry response.

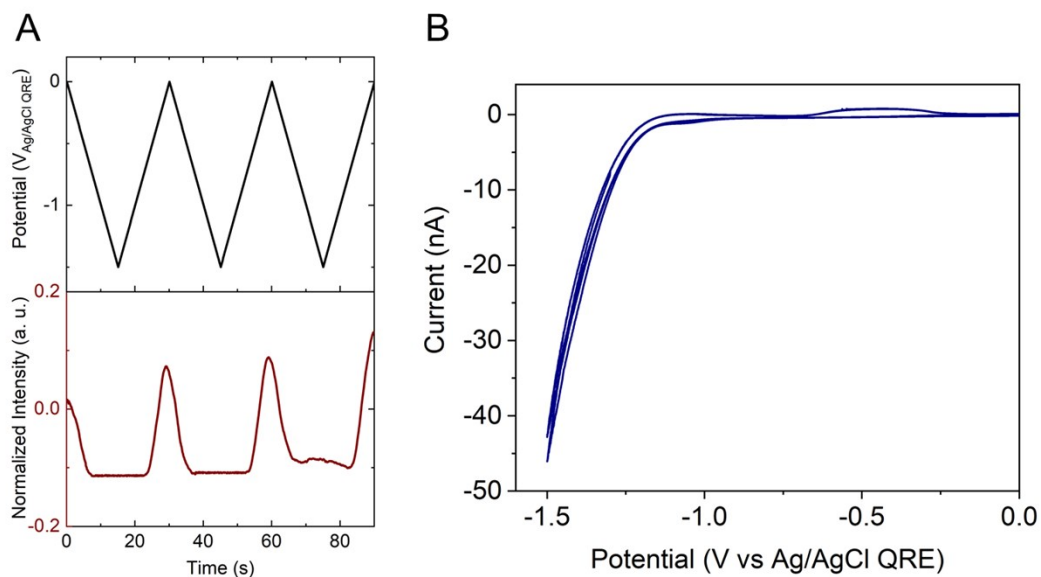


Figure S11. (A) Applied potential waveform as a function of time (*top*) and corresponding individual fluorescence normalized intensity – time traces (*bottom*) for one E-ZMW nanopore. The initial pH of the solution is pH 3 with 3 μM redox-active Alexafluor 488 and 0.2 M KNO_3 . (B) Corresponding cyclic voltammetry response over 3 cycles.